Bollettino di Geofisica Teorica ed Applicata Vol. 55, n. 2, pp. 281-302; June 2014
DOI 10.4430/bgta0086

Microseismicity and crustal deformation of the Kyparissiakos Gulf, south-western Hellenic Arc, using an "amphibious" seismic array and a 3D velocity model obtained from active seismic observations

J. Papoulia[1], J. Makris[2] and A. Tsambas[1]

[1] *Hellenic Centre for Marine Research, Institute of Oceanography, Athens, Greece*
[2] *University of Hamburg, Germany*

(Received: March 1, 2011; accepted: December 12, 2012)

ABSTRACT In Fall 2006, in the frame of the European Community SEAHELLARC project, we deployed an "amphibious" seismic array consisting of 17 3-channel stand alone stations onshore and 17 4-channel ocean bottom seismographs in the Kyparissiakos Gulf and surrounding area of western Peloponnese. We observed the microseismic activity for a period of two months. The geometry and location of the array were designed to particularly observe the offshore activity and define the continuation of known onshore active faults offshore. Data evaluation and location of the seismic events were accomplished in three steps, successively improving the location accuracy. First we used the standard procedure for foci location with a 1D velocity model and the Hypoinverse algorithm. Locations were then improved by 3D passive tomography, using P and S arrivals. The optimum solution of the seismic foci location was finally achieved by using a 3D velocity model developed from active seismic observations and 3D gravity modelling. More than 3500 earthquakes over a threshold magnitude of 0.3 M_D were identified, using arrivals from a minimum of six stations per event. Shallow seismicity is confined mainly onshore Zakynthos Island, at the continent-ocean transition to the west, and in the area of Pylos - Messinia. These zones are deforming by westward thrusting of the Alpine napes and collision of the continental backstop of pre-Apulia with the Ionian oceanic lithosphere at the Mediterranean Ridge. Deeper seismicity follows the subduction of the Ionian lithosphere below western Peloponnese with successively increasing hypocentre depths eastwards. A cluster of subcrustal events extending to 90 km depths is located in a pull apart basin NE of Strofades Island in the forearc. These events also generated T-phases. We attribute this "unusual" seismicity to lateral deformation and fracturing of the oceanic lithosphere during its subduction below a continental crust of laterally varying thickness.

Key words: Hellenic Arc, Kyparissiakos basin, Greece, microseismicity, crustal deformation, T-phases, SEAHELLARC.

1. Introduction

Aim of the SEAHELLARC [SEismic and tsunami risk Assessment and mitigation scenarios in the western HELLenic ARC: see Papoulia *et al*. (2014)] project was to develop a new approach in assessing seismic and tsunami hazard by exploiting new hardware and combining geological, geophysical and engineering studies. The south-western part of the Hellenic Arc, was used as a pilot area, since it is one of the most seismically active zones in Greece and the entire Mediterranean region (e.g., McKenzie, 1972; Makropoulos, 1978; Makropoulos and Burton, 1981; Jackson and McKenzie, 1988). This area has been repeatedly affected by large magnitude earthquakes (i.e., 1886 Filiatra *M* 7.3, 1893 Zakynthos-Keri *M* 6.5, 1899 Kyparissia *M* 6.5, 1947 Pylos *M* 7.0, and 1997 Gargaliani *M* 6.6) that have caused severe destruction and human loss (Papazachos and Papazachou, 1997), and, occasionally, local but destructive tsunamis (Soloviev, 1990; Papazachos and Dimitriu, 1991). Despite the significant progress in construction and earthquake engineering standards, the population growth and extensive urbanization of western Peloponnese have caused the risk from earthquakes and tsunamis to increase significantly. This situation requires a reliable seismic hazard assessment and effective risk management and mitigation plans. For this purpose, it is essential to study the local seismic activity and define active fault zones onshore and offshore with high accuracy and resolution required for a reliable seismic and tsunami hazard assessment. These questions were addressed during the SEAHELLARC project.

To better constrain the microseismic activity and associate it with local tectonics, we deployed an on/offshore seismic array in the Kyparissiakos Gulf and surrounding coastal regions of western Peloponnese, Zakynthos and Strofades (see Fig. 1). The study area is approximately 5000 km^2 large. Average spacing of the stations was 1 per 147 km^2. Both marine and land stations were equipped with SEDIS III seismic recorders developed by GeoPro, Hamburg (Makris and Moeller, 1990). This instrument can be used offshore integrated in an Ocean Bottom Seismograph (OBS) or as a stand-alone seismic station onshore. The OBSs, (see Fig. 2) is a 4-channel recording station with a 30 GB hard disc or 16 GB storage capacity on flash memory, a dynamic range of 120 dB at 250 Hz sample rate. Timing is obtained by a GPS receiver and also by an inbuilt thermo stabilized quartz clock of 10^{-8} accuracy and strictly linear drift. Electronic components and sensors are housed in a 17 inch glass sphere that withstands pressure corresponding to more than 6000 m water depth. Broadband sensors (60 s – 30 Hz) or 4.5 Hz geophones can be deployed with the SEDIS system (see also www.geopro.com).

The "amphibious" SEAHELLARC array operated for two months, from September 23 to November 26, 2006. For the OBS stations we used alkaline D-size batteries that allow continuous monitoring for approximately 25 days, thus we had to retrieve them twice during the survey. Onshore stations were equipped with solar panels (see Fig. 3) and batteries that permit continuous operation throughout the whole observation period.

More than 3500 microearthquakes were located in the Kyparissiakos Gulf and its vicinity. Accuracy of the seismic foci was optimized by applying a 3D velocity model developed from 2D active seismic observations and 3D gravity modelling, converting *Vp* velocities into densities and vice versa, by means of the empirical functions of Birch (1960, 1961) and Nafe and Drake (1963). In the following we present the results of the SEAHELLARC "amphibious" seismic experiment, and discuss them in connection with the tectonic evolution of the western Hellenides.

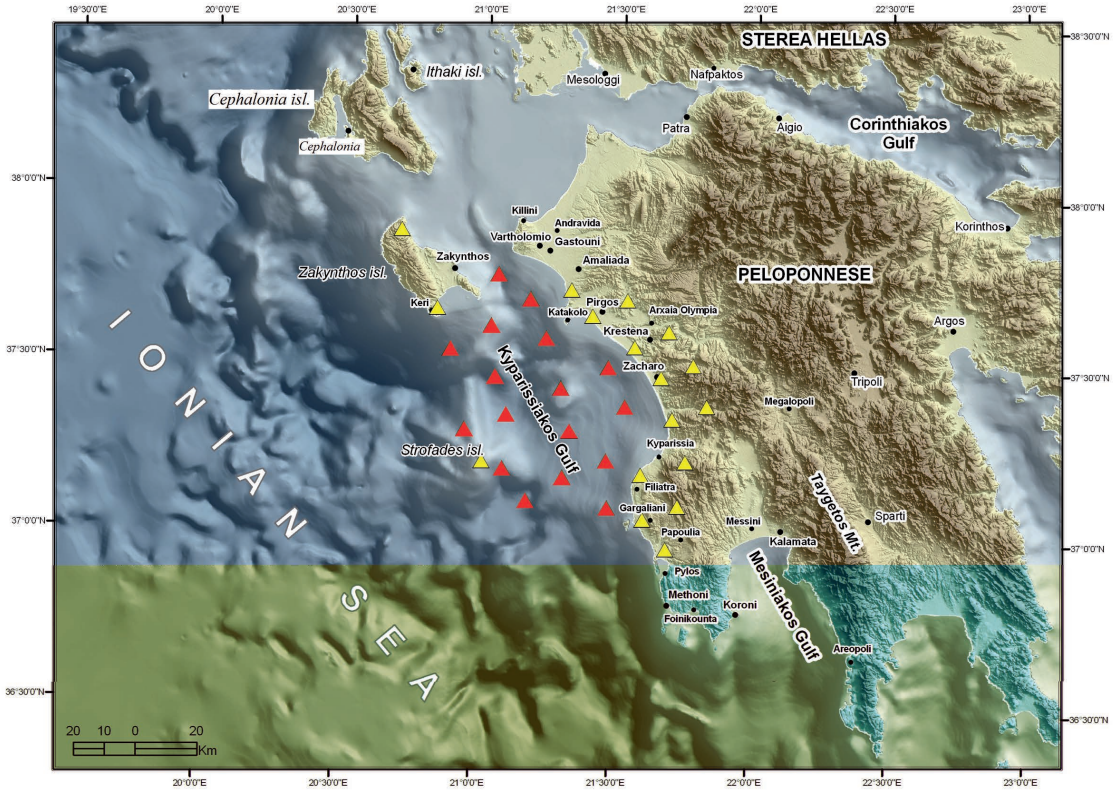

Fig. 1 - The "amphibious" SEAHELLARC seismic array consisting of 17 OBSs (red triangles) and 17 land stations (yellow triangles). Operational period: September 23 – November 26, 2006.

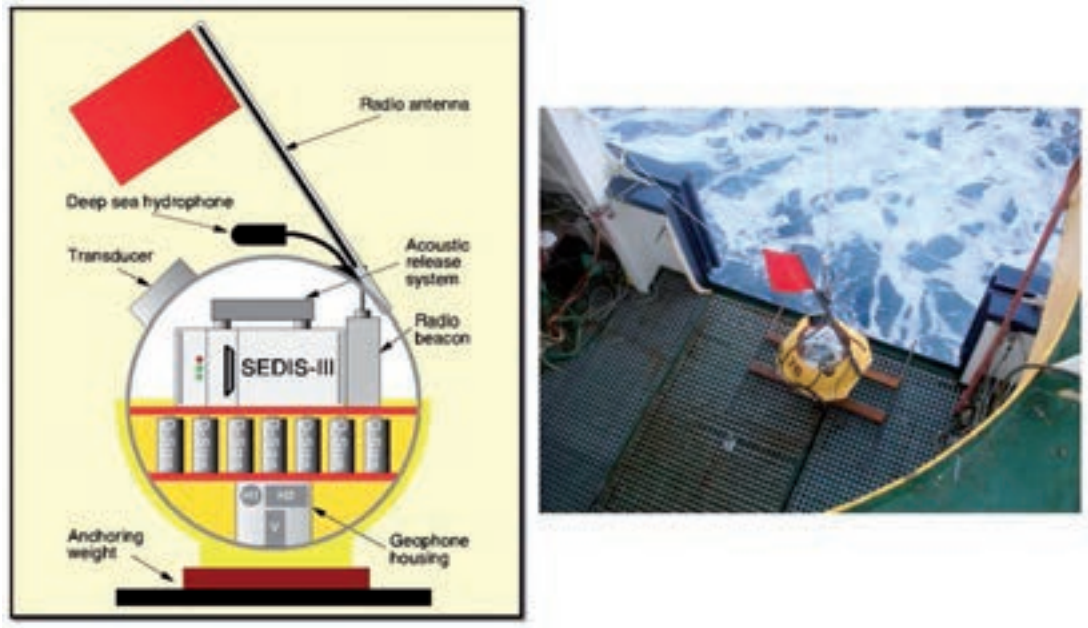

Fig. 2 - The GeoPro OBS. Schematic reconstruction of components contained in a 17 inch glass sphere (left). OBS with anchoring weight on research vessel (R/V) AEGEAO-HCMR ready for deployment (right).

Fig. 3 - The GeoPro stand alone seismic station contained in a waterproof plastic box (left). The station has 6 channels and can record for 1 month on alkaline D-size batteries or continuously with solar panels (right).

2. The recorded seismicity and its evaluation

Evaluation of the seismicity data was performed using a semi-automated procedure. The detection of seismic events was achieved using the ratio of short to long time average (STA/LTA) of noise and seismic energy (Urabe and Hirata, 1984). The threshold level for this operation is variable and can be selected as required. Correlation of detected arrivals was accepted if each event was identified at a minimum of six stations. For each identified event we picked P and S arrivals, the coda length for magnitude and the first motion polarity for focal mechanism definition.

Data evaluation and location of the seismic events were completed in three steps, by applying: 1) the standard 1D velocity model and the Hypoinverse code (Klein, 1989), 2) a 3D velocity model from passive tomography and simultaneous inversion of P and S arrivals (Thurber, 1983), and 3) a 3D velocity model developed by active seismic observations and 3D gravity modelling. As described in the following sections RMS travel time residuals were successively improved from the first to the last evaluation step, and the reliability of locating seismic events and identification of active faults significantly increased.

For the initial location of seismic foci, we used an 1D velocity model (Table 1), averaged from active seismic observations (Makris and Papoulia, 2009).

Magnitudes were defined by coda lengths of the recorded seismograms, calibrated by local earthquakes that had been recorded also at the seismograph network of the National Observatory

Table 1 - Local velocity model for hypocentral location (after Makris and Papoulia, 2009).

Velocity *Vp* (km/s)	Depth (km)
4.5	0.0
6.2	4.0
6.8	10.0
8.0	25.0

of Athens, applying the Crosson (1972) method. Calibration functions were defined at four reference stations of the array:

$$P_{15} : M_D = \quad 0.2658 - 0.0010 \times D + 1.6305 \times \log T$$
$$P_{21} : M_D = -1.8020 - 0.0012 \times D + 2.8366 \times \log T$$
$$P_{26} : M_D = -0.9945 - 0.0009 \times D + 2.3120 \times \log T$$
$$P_{31} : M_D = -0.3846 - 0.0012 \times D + 2.0201 \times \log T$$

where D is the epicentral distance in km between a given station and the epicentral location of the event, and T is the coda length of the recorded event, measured at the seismogram of the vertical component.

In two months (September 23 to November 26, 2006), we located 3508 events above a threshold magnitude of M_D 0.3 by applying Geiger's (1912) method, observed by a minimum of six stations. During the first half of the observation period seismicity was more intense, having a maximum of 138 events on October 1, 2006 (see Fig. 4). The threshold magnitude of completeness is M_D 2.8 as indicated from the first derivative's maximum value in the frequency-magnitude plot, based on the assumption of the Gutenberg-Richter relationship (see Fig. 5).

The "unusual" seismicity distribution of Fig. 4 is the result of a large number of more than 2400 events spatially confined within a narrow zone, NE of the Island of Strofades. These events had focal depths exceeding 90 km also genereting T-phases that were located using a minimum

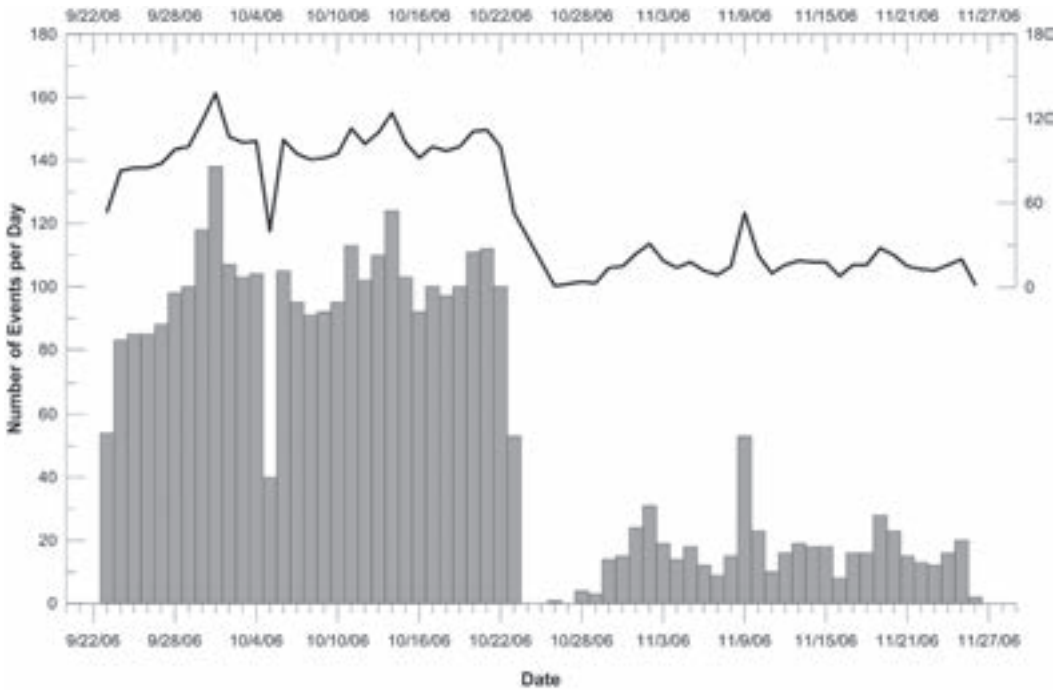

Fig. 4 - Variations of the seismic activity from September 23 to November 26, 2006 (solid line) and distribution of events per day (bar chart) in the Kyparissiakos Gulf, western Peloponnese. Seismic activity was significantly reduced after October 24 to an average of approximately 10 events per day.

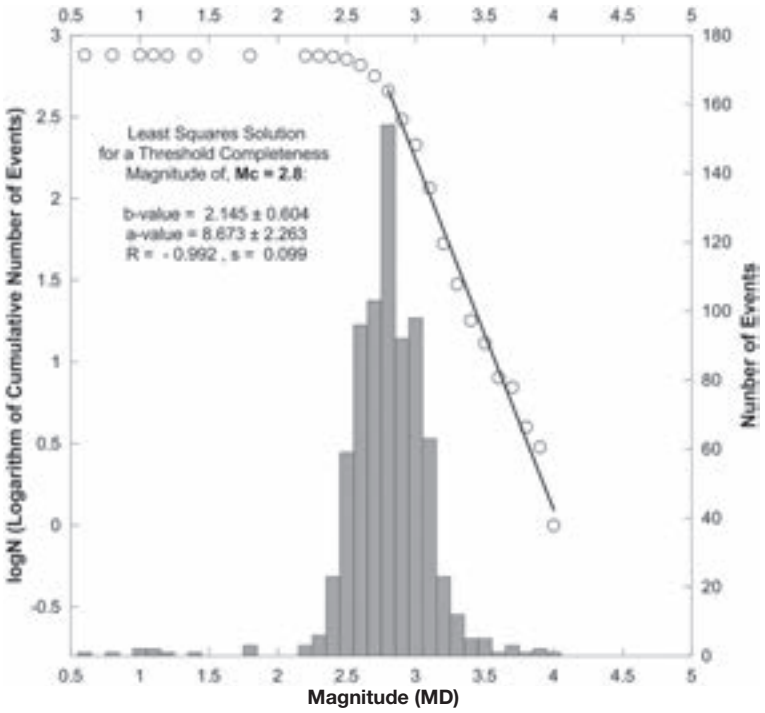

Fig. 5 - Completeness magnitude estimation and frequency - magnitude distribution according to the Gutenberg-Richter relationship for $M_D \geq M_c$.

of 5 OBS stations. An example of a T-phase recording is given in Fig. 6. The propagation mechanism of T-phases is linked with the acoustic transmission of seafloor vibrations through the SOFAR channel. Since T-phases can transmit energy from small events over large distances very efficiently and with hardly any attenuation, they provide an exceptional opportunity to detect and locate small events, which would otherwise have gone undetected (see Okal, 2008). We attribute this "unusual" seismic activity to lateral deformation and fracturing of the Ionian oceanic lithosphere during its subduction below a continental crust of laterally variable thickness (see also Makris and Papoulia, 2014). Exploiting T-phase observations can give a better insight on seismic source properties and fracturing processes. This, however, is beyond the scope of the present study, and will not be further elaborated.

The RMS travel time residuals of the first evaluation step (1D local velocity model) for all located events, inside and outside the seismic array, had an average value of 0.17 s. This corresponds to an epicentral accuracy of ±2 km. The focus depths are affected by an error twice this value for events located within the crust. Outside the network location errors are significantly higher than those inside the array, and this influences the RMS value presented here. This will be further discussed below. Within the same observation period, the seismograph network of the National Observatory of Athens (GI-NOA) recorded only 104 events with magnitudes M_L ranging from 2.9 to 4.1. This emphasizes the importance of using local seismic arrays for accurately mapping microseismicity and identifying active faults for seismic hazard and engineering applications. Using regional zonation models for hazard, estimation can lead to significant errors.

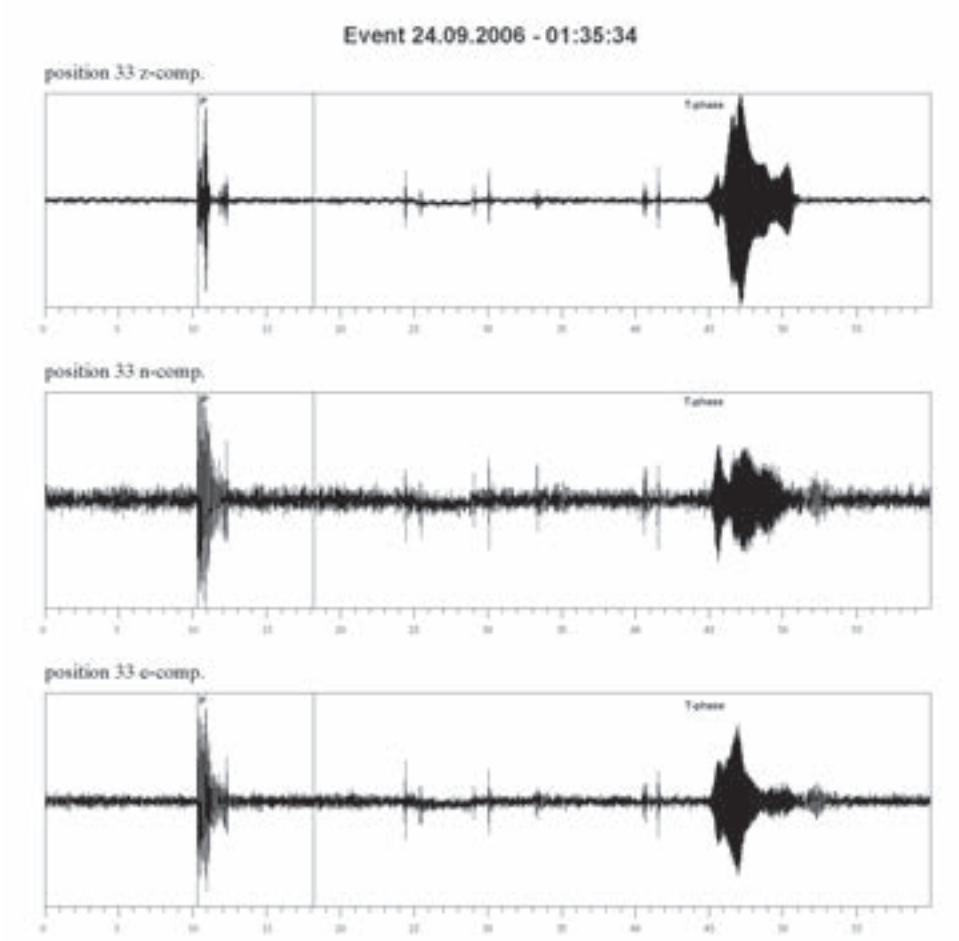

Fig. 6 - Seismic event recorded at an OBS station showing also T-phases. Time scale is in seconds. We recorded more than 2400 T-phase events of very good quality in nearly one month.

A first improvement of the foci locations and also a first approximation of a 3D velocity model were achieved by using passive tomography and the SIMULPS14 procedure (Thurber, 1983). This technique is extensively useful improving the location of the seismic foci and provides a 3D velocity model, helping to understand crustal properties. The RMS value of the residual travel times is significantly improved. The method was originally developed by Thurber (1983), and was optimized by Eberhart-Phillips (1986, 1990).

From the initially located events we extracted 593 observed by a minimum of 10 stations and these events were selected for passive seismic tomography. Both P and S wave arrivals were inverted with the VELEST algorithm (Kissling *et al.*, 1994), and an initial 1D velocity model was generated that extends to 50 km depth (see Table 2). This 1D velocity model was used as initial input for the SIMULPS14 procedure, thus restricting the solution space.

The P- and S-wave velocity values obtained as a function of depth after finalizing the 3D simultaneous inversion are presented in Figs. 7 and 8. Grid values of the resolution matrix (KHIT) at the corresponding depths are given in Fig. 9. The first cross-section at 1 km shows that the basin of Kyparissiakos is flanked to the south and north by two uplifted basement blocks. The central part is filled with sediments of 3.5 km/s velocity. At 4 km depth, the basin

Table 2 - Parameters of the grid and velocity values used as input for the SIMULPS14 procedure.

Depth (km)	Nodes NE	Nodes SW	Initial P Velocity (km/s)	Initial S Velocity (km/s)
0.0	5	7	4.22	2.37
1.0	5	7	4.73	2.66
4.0	5	7	5.21	2.93
6.0	5	7	5.79	3.25
8.0	5	7	5.95	3.34
13.0	5	7	6.12	3.44
23.0	5	7	6.88	3.86
35.0	5	7	7.50	4.21
50.0	5	7	8.15	4.58

structure is even better accentuated. The basin flanks to SE and NW have velocities between 5.6 and 6.0 km/s, while the central part is filled with sediments having velocities between 3.5 and 4.5 km/s. This trend is also valid for the 6 km depth level showing the uplifted blocks to the SE and NW at their full extend, while the central part of the basin is still filled with material of relatively low velocity not exceeding 5.0 km/s. At the 8 km depth level the northern and southern flanks show that crustal rocks are now limiting the basin and that only a central thin belt is still filled with sediments. Between 13 and 23 km depth the *Vp* velocities correspond to intracrustal conditions while offshore Messinia at 23 km we have already reached the upper mantle with V_p velocity of 8.0 km/s. S-wave observations further constrain the P-wave results and confirm the sediment and crust models. (Fig. 8). In summary, passive seismic tomography revealed successfully the main geometry of the Kyparissiakos basin and the crust below it and significantly increased the relocation accuracy for the focus depths.

3. A 3D velocity model constrained by gravity and seismic data: input for improving the hypocentral locations

In order to improve the accuracy of the foci locations, we re-evaluated the recorded events using an independent 3D velocity model. This was developed by combining 2D velocity models of the crust and sediments from active seismic experiments (Makris and Papoulia, 2009; Papoulia and Makris, 2010) with 3D density modelling constrained by the Bougeur gravity field of western Greece (Makris, 1977; Makris and Morelli, 1994; Makris *et al.*, 1998). The procedure followed is briefly described below.

First we developed 2D density models along the seismic profiles located in south western Greece. Accuracy of sediments and crustal thickness is ±5% (Makris *et al.*, 2013). The V_p velocities were converted into densities using the empirical functions of Nafe and Drake (1963) for the sediments, and Birch (1960, 1961) for the crustal rocks. The 2D density sections constrained the initial 3D density model for 3D gravity computations. This procedure was continued until the best fit between observed and synthetic gravity values was obtained (Makris and Yegorova, 2006; Makris *et al.*, 2013).

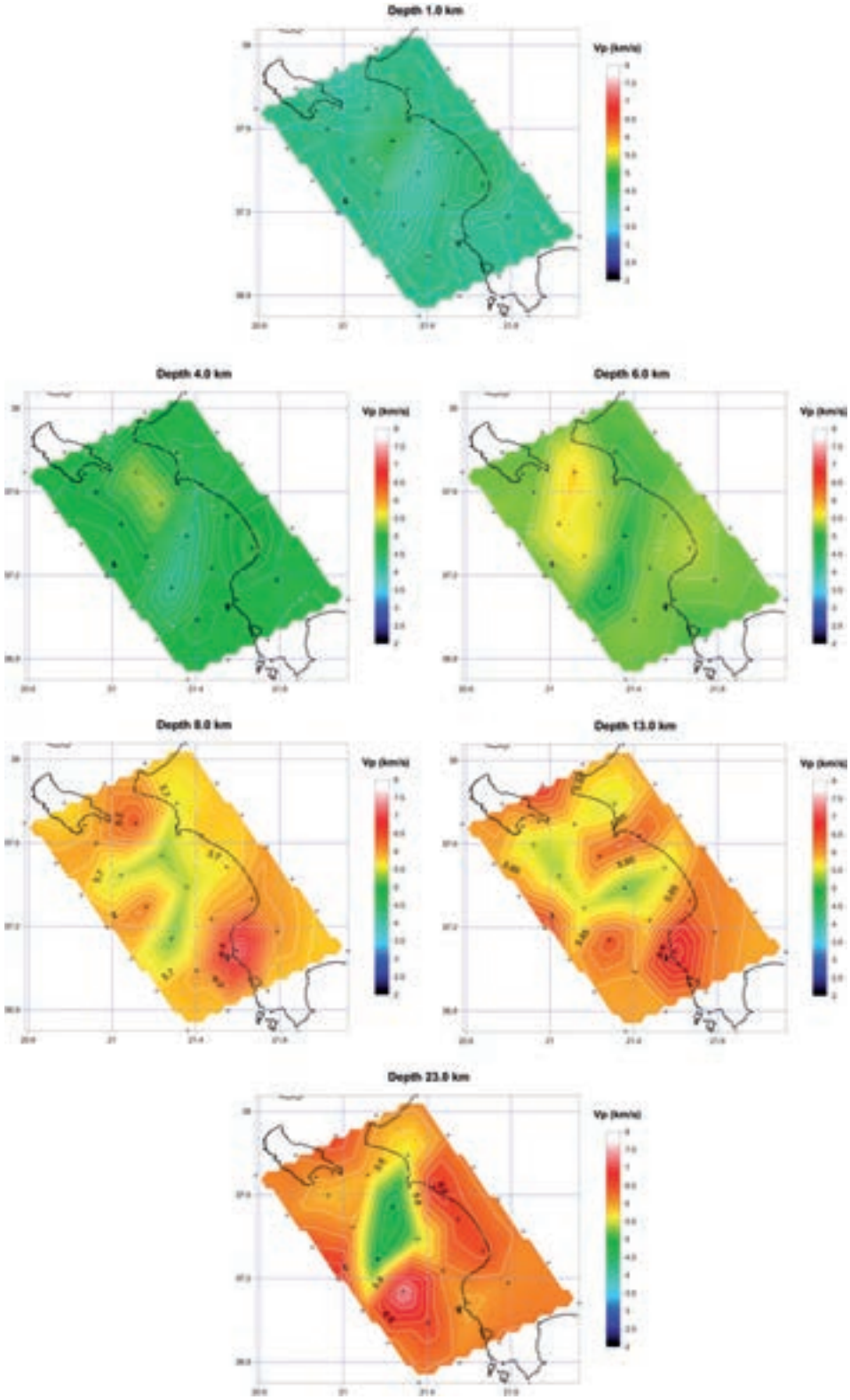

Fig. 7 - The 3D velocity model (P-wave values) developed by passive tomography are presented for 6 levels cutting through the 3D velocity volume. Discussion in text.

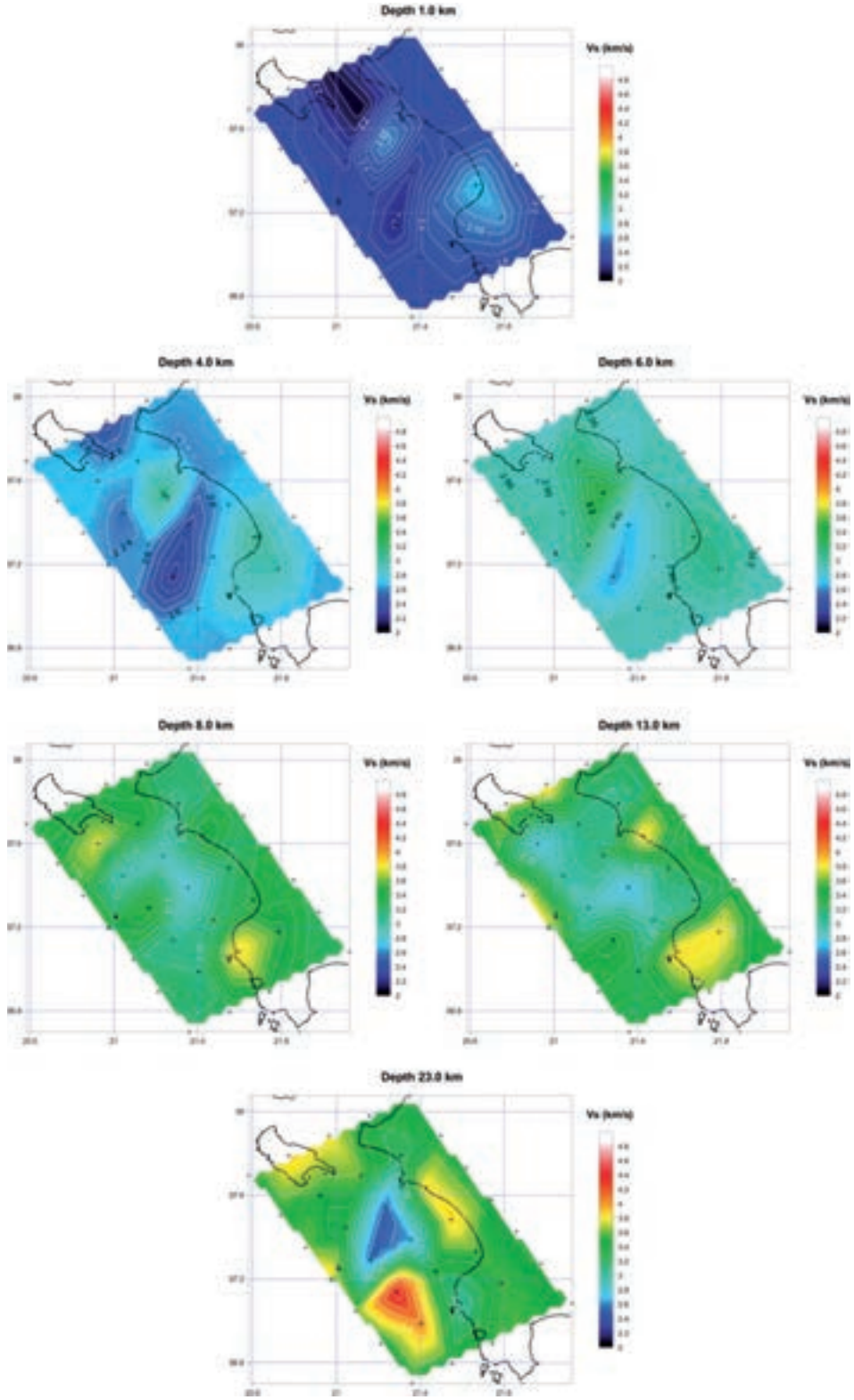

Fig. 8 - The 3D velocity model (S-wave values) developed by passive seismic tomography is presented for 6 levels cutting through the 3D velocity volume. Discussion in text.

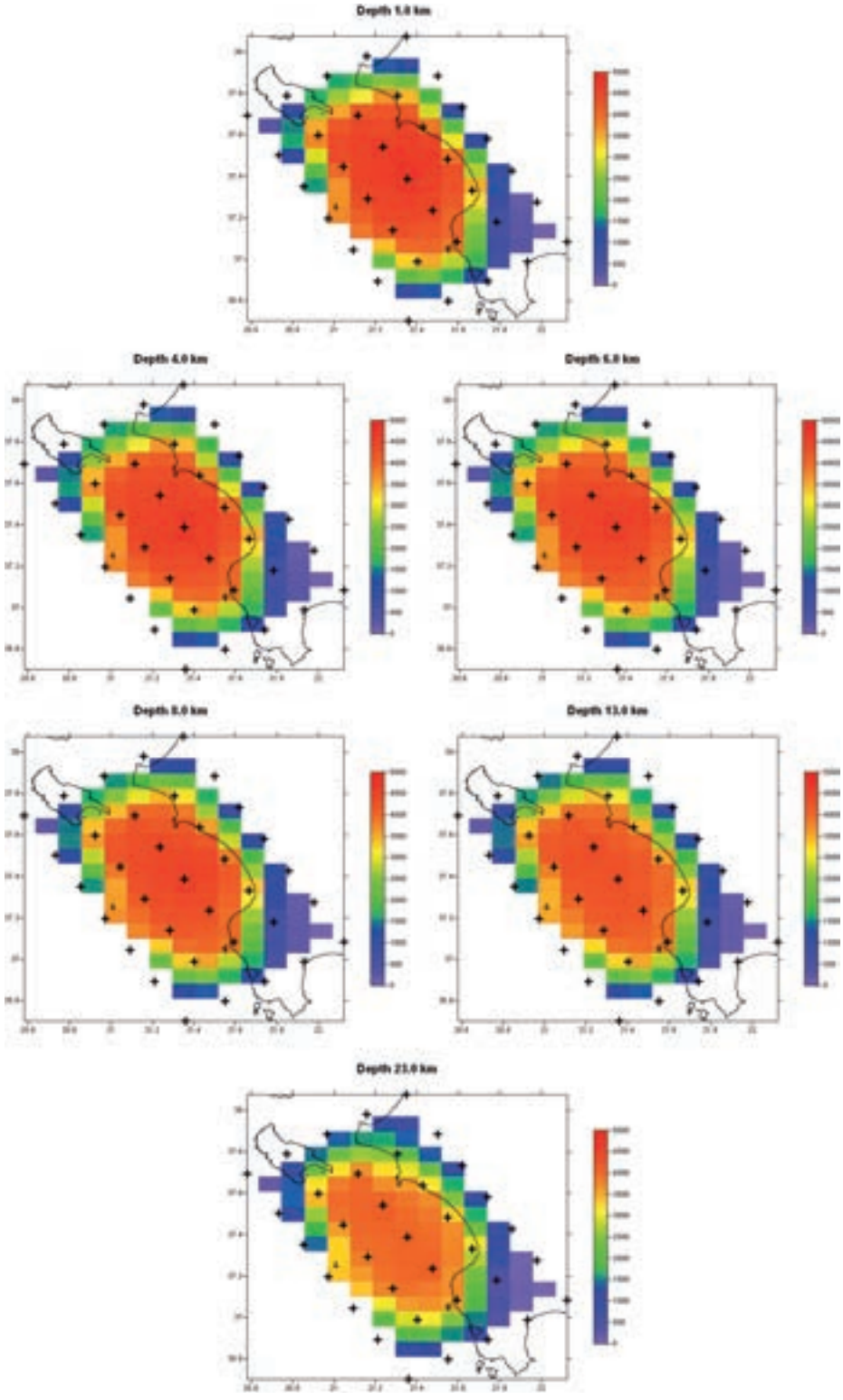

Fig. 9 - The resolution matrix at the corresponding 6 levels of the velocity distribution shows that the velocity model is very well constrained by the seismic data at the central part of the area. The seismic array covers homogeneously this part of the Kyparissiakos Gulf.

The final 3D density model was converted into a 3D velocity model by applying again the above mentioned empirical functions. In Fig. 10 we present the 6 km/s and the 8 km/s interfaces of the 3D velocity model. The lateral variations of the sediments and crust are very intense, since the area is rapidly deforming by crustal shortening in a continent/ocean collision. This is expressed by the presence of high seismic activity and intense tectonization. A better visualization of the relationship between topography-bathymetry, basement geometry and crustal thickness, is given in the 3D picture of Fig. 11. It shows that under the high elevations of western Greece and the Peloponnese the sediments and Moho are depressed and the crust obtains its maximum thickness. Under the eastern Ionian Sea, where the bathymetry has its maximum values, also the basement depth obtains its maximum depression. Lateral velocity and density variations are very intense and it is impossible to accurately define focus locations using 1D velocity models. Therefore, locations of the seismic foci can only be reliably obtained, and consequently have practical value for seismic hazard analysis, if they are evaluated using a 3D velocity model.

The velocity volume restricted by the two surfaces, the topography – bathymetry, and a plane surface at 50 km depth determine the modelling space, which is discriminated by prisms of 5 x 6 km elements. The relocation of the foci was obtained by maintaining the velocity model constant and perturbing the foci locations until the best fit between observed and calculated travel times was achieved. For this purpose we used again the SIMULPS14 tomographic inversion procedure. The advantage of this inversion is that the process is now linearized by maintaining the velocity model constant and perturbing only the foci locations. The final solutions of the focus locations are quickly obtained, since the residual times decline rapidly to the limiting value defined by the picking accuracy.

4. Relocation accuracy of seismicity using an independent 3D velocity model

The 3D velocity model derived from 2D active seismic experiments and gravity modelling as previously stated was used to relocate the seismic foci. To demonstrate the importance of the velocity model on the accuracy of hypocentral location, we present a comparison of the RMS residual travel times obtained from the various velocity models (see Fig. 12). We only considered a selected data set of 593 events located within the seismic array and were used for the passive tomography. Average RMS is 0.08 s, using the 1D Hypoinverse location. It decreases to 0.06 s, after the simultaneous inversion and relocation from the 3D passive tomography. The minimum RMS value of 0.04 s is obtained after the final relocation using the independent 3D velocity model from 2D active seismic observations and 3D gravity modelling. Crustal seismicity can now be located within 500 to 700 m, depending on the depth of the event. This permits to locate active faults within the crust and sediments with sufficiently high accuracy as it is needed for seismic hazard engineering applications.

5. Seismicity, focal mechanisms and active tectonics

The distribution of seismic activity using the independent 3D velocity model from active experiments and 3D gravity modelling is presented in Fig. 13. The seismic bulletin of the

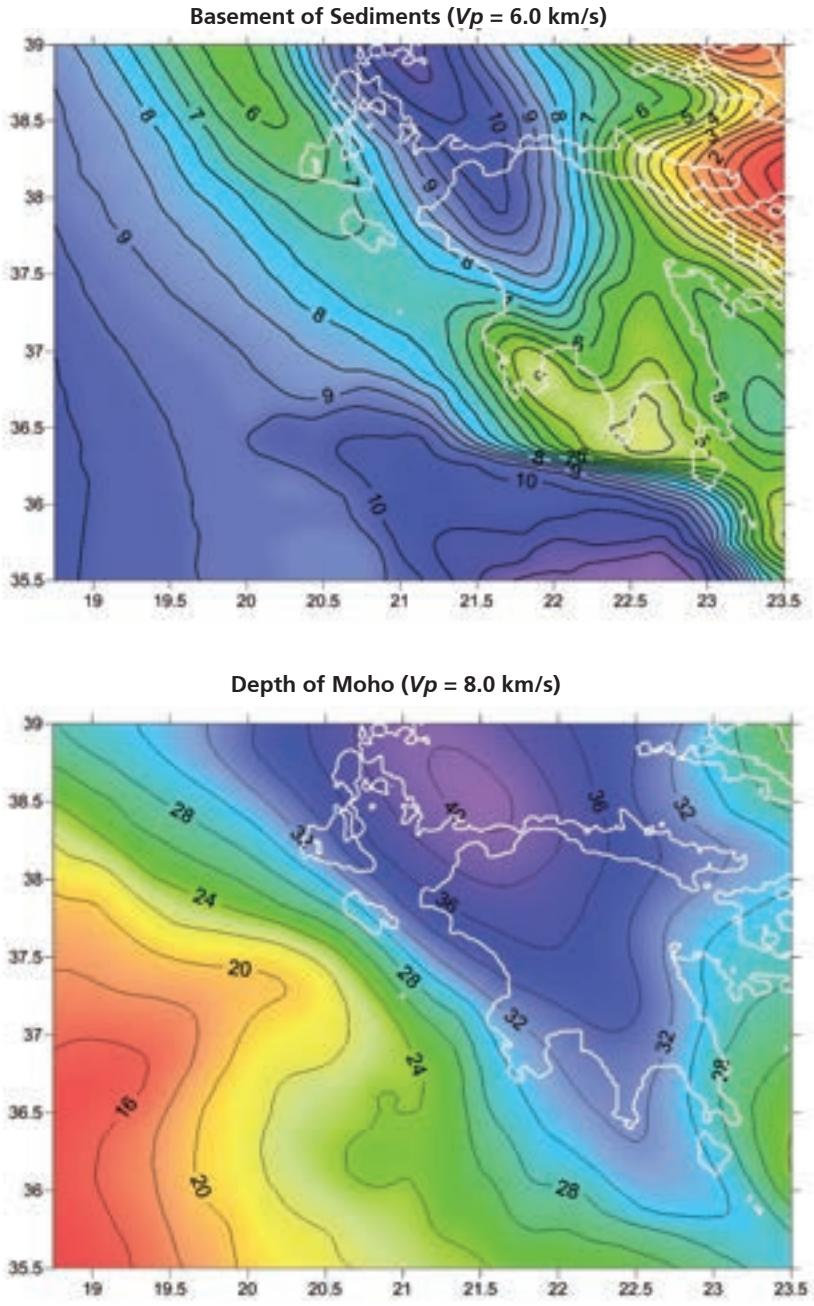

Fig. 10 - Depth to basement (upper part) and crust (lower part) in km for south-western Hellenic Arc.

seismic events is given in Annex 1 (at www2.inogs.it/bgta).

Focal mechanisms of selected events were determined using the FPFIT code (Reasenberg and Oppenheimer, 1985) using the observed P-wave polarities. The code calculates the double-couple fault plane solution (source model) that best fits a given set of observed first motion polarities for one single event. A summary of 105 most reliable fault plane solutions is given in Annex 2 (at www.2.inogs.it/bgta).

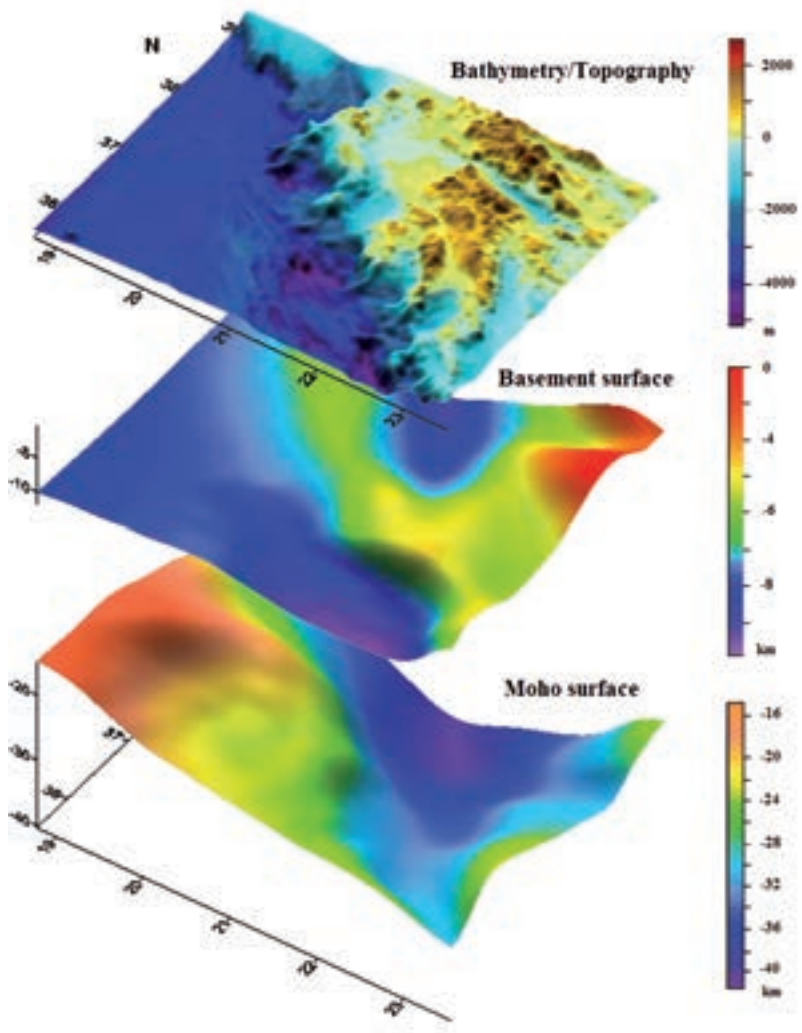

Fig. 11 - 3D presentation of the topography-bathymetry (top), basement geometry (middle) and crustal thickness (bottom) in the south western Hellenic Arc.

Combining the results of microseismicity with active seismic observations (Makris and Papoulia, 2009; Papoulia and Makris, 2010; Makris and Papoulia, 2014) and high resolution swath mapping (Camera *et al*., 2014), we developed a tectonic map of the Kyparissiakos Gulf and surrounding area (see Fig. 14). Onshore faults are taken from the publication of IGME (1989).

Two major clusters of seismic activity are associated with the NNW-SSE trending faults onshore Zakynthos Island and in the continental backstop to the west. Fault plane solutions show extension with strike slip movements (see Fig. 15), and are associated with the extensional basins behind the NNW-SSE thrust fronts.

Intense seismicity is also observed SE of Cephalonia Island, correlating with a major NW-SE trending fault system onshore Cephalonia and north-western Peloponnese.

Messinia and its coastal areas are tectonized by normal faulting of N-S and E-W orientation that generates horsts and grabens [see also Papoulia and Makris (2004) and Papanikolaou *et al*. (2007)]. Fault plane solutions show normal and thrust movements with strike slip component for

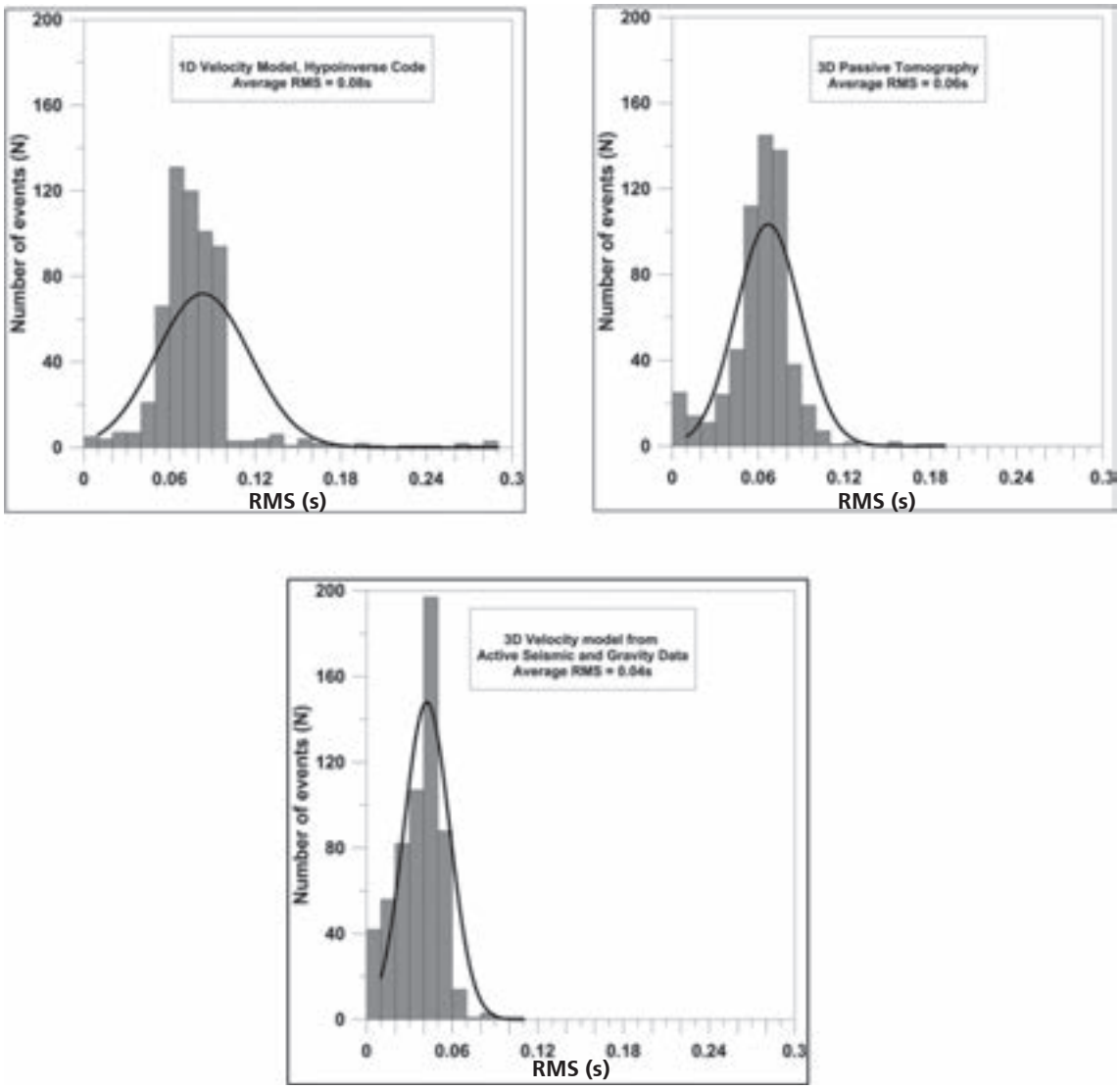

Fig. 12 - Comparison of RMS distribution for a selected data set of 593 events according to the initial 1D Hypoinverse (left above) location, a relocation using a 3D velocity model from passive tomography (right above) and a relocation using and independent 3D velocity model from active seismic observations and 3D gravity modelling (bottom). Mean values of the travel-time residuals improved from initial 0.08 s (1D Hypoinverse), to 0.06 s (passive tomography relocation) and to 0.04 s (relocation using a pre-defined 3D velocity model from active seismic results).

many of the areas described above (see Fig. 15). It is therefore obvious that in the frontal area of continental crust shortening and the subduction of the Ionian oceanic lithosphere below western Greece the deformation is very complex and over simplifications of regional models cannot be used for engineering applications. Local deformation can be delineated reliably only by using local networks adjusted to the engineering requirements.

The deeper seismicity (at the lower crust/upper mantle boundary) follows the subduction of the oceanic Ionian lithosphere below western Peloponnese with constantly increasing hypocentral depths eastwards.

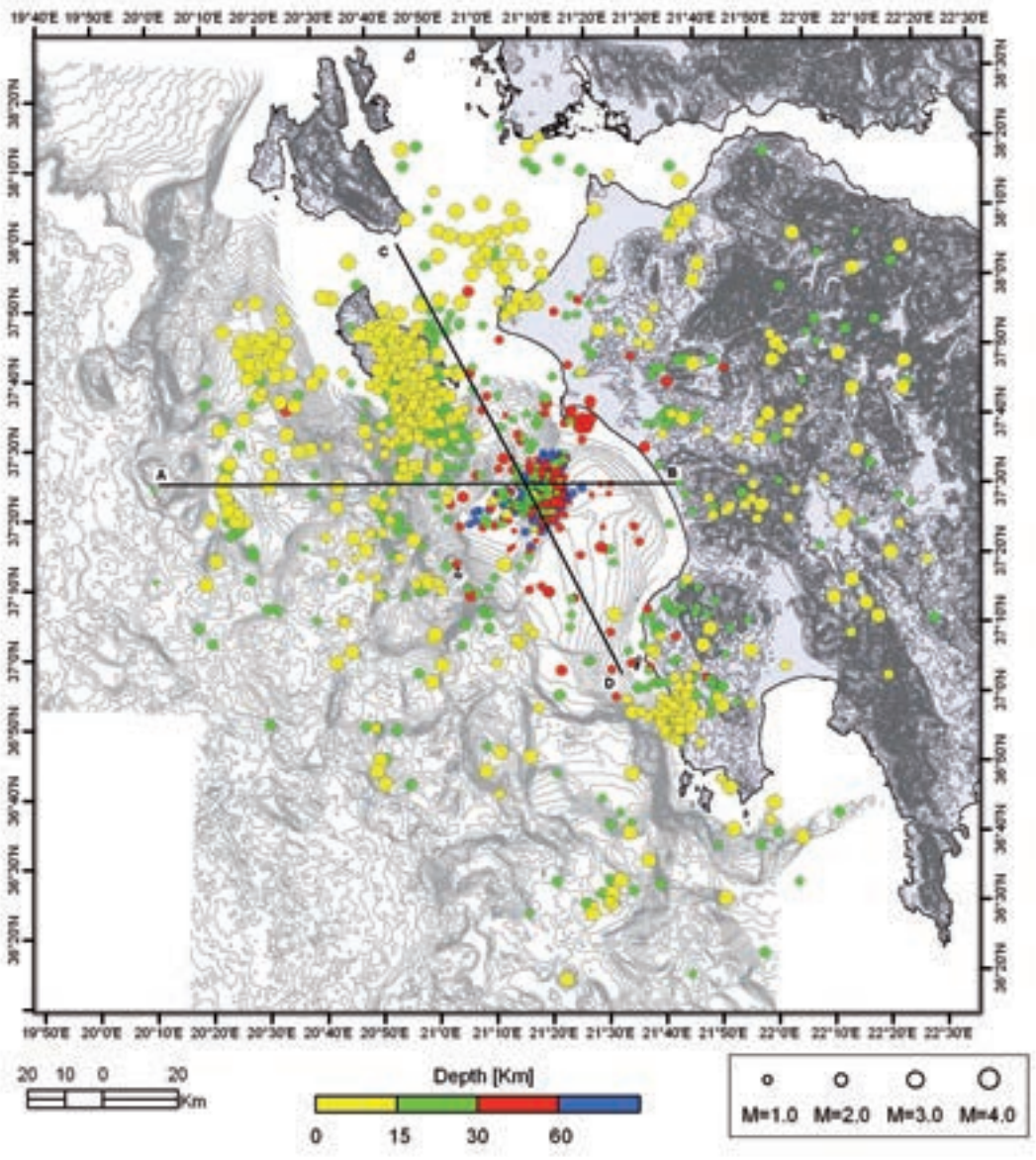

Fig. 13 - Seismicity recorded by the SEAHELLARC "amphibious" seismic array using a 3D independent velocity model defined from 2D active seismic experiments and 3D gravity modelling. Further explanations in the text.

A significant number of seismic events with depths exceeding 90 km were recorded at the central part of the Kyparissiakos Gulf (see also Fig. 16). This spatially confined seismicity correlates with a transtensional basin NE of the Island of Strofades (Camera *et al*., 2014), linked to the Andravida dextral strike slip fault system. We attribute this deep seismicity to fracturing of the oceanic lithosphere due to differential bending of the subducted slab below a continental crust of laterally variable thickness. Focal mechanisms associated with this zone show dextral strike slip deformation and the wrench faults are oriented perpendicular or near perpendicular to the collision front.

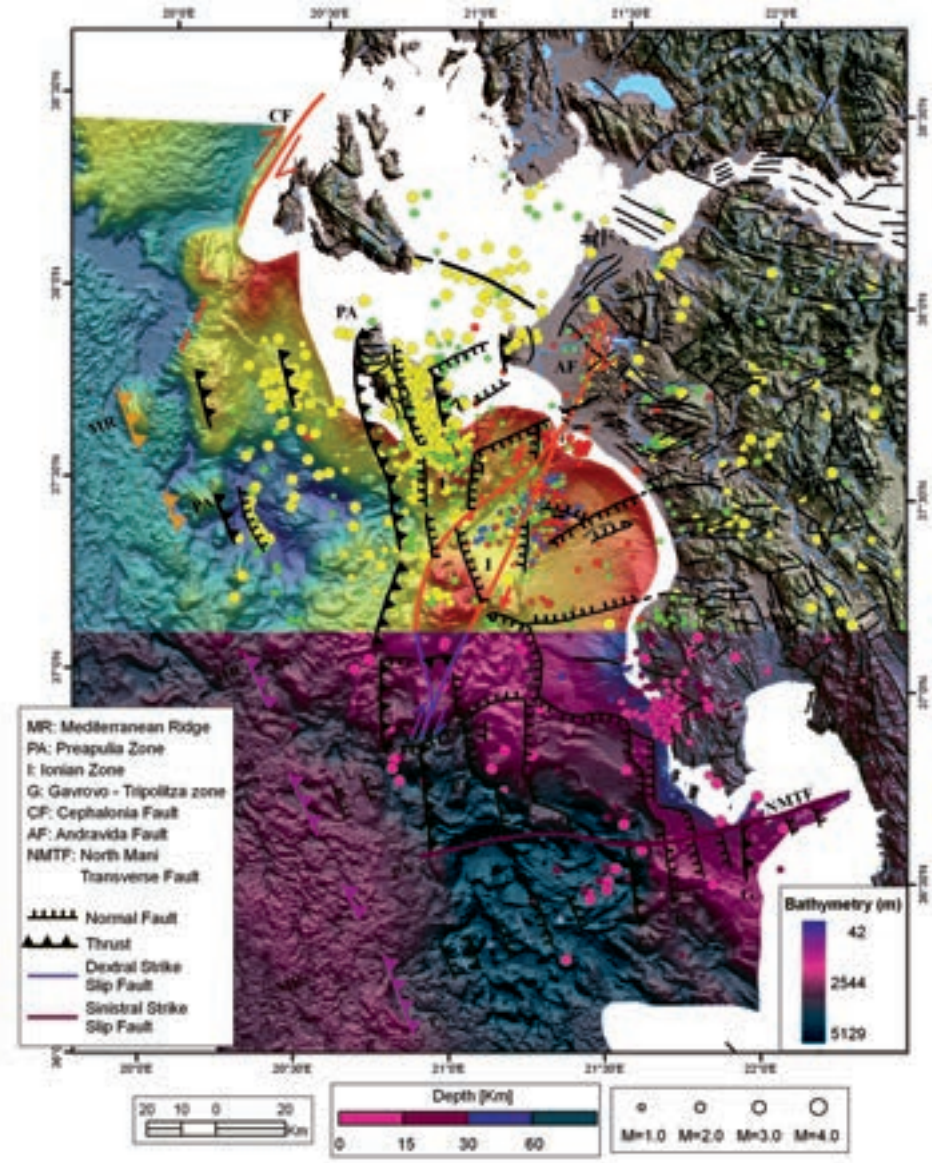

Fig. 14 - Microseismicity distribution and tectonic model of the Kyparissiakos Gulf and surrounding area. Further explanation in text.

To better demonstrate the relation between local tectonic structures and microseismicity, we plotted two cross-sections, across and parallel to the main geological features. All events located 10 km on either side of the 2D profiles were projected into the cross-sections.

Profile AB, of E-W orientation (see Fig. 17), crosses from the deep Ionian Sea, offshore south Zakynthos and NE of Strofades, towards Peloponnese. At km 10 along the profile a cluster of seismic activity correlates with a normal fault in the backstop area, approximately 30 km east of the Mediterranean Ridge. The next significant cluster between km 52 and 75 coincides with the Zakynthos-Strofades uplift, built by the lower limestone of the pre-Apulian zone (Makris

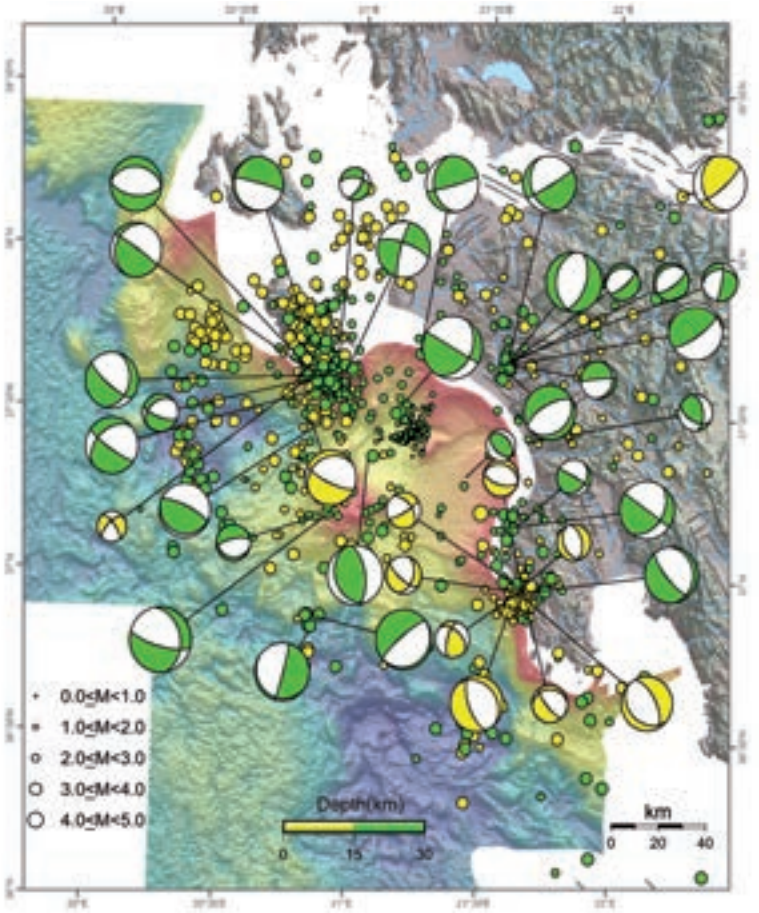

Fig. 15 - Fault plane solutions for events with focal depths less than 15 km (yellow) and between 16 and 30 km (green).

and Papoulia, 2009). Between km 90 and 100 a significant seismic cluster of subcrustal activity, with depths exceeding 90 km coincides with the pull apart basin NE of the Strofades Island. The subduction of the Ionian oceanic lithosphere below the continental crust of Peloponnese is clearly expressed along the profile by the successive increase of the hypocentral depths eastwards. Crustal thickness constrained by active seismic observations (Makris and Papoulia, 2009) is indicated in the cross-section.

Profile CD, of NNW-SSE orientation (see Fig. 18), strikes parallel to the Peloponnese coast, from offshore Zakynthos to offshore Messinia. The Kyparissiakos Gulf is flanked by two uplifted blocks, that of Zakynthos to the NW, and Pylos to the SE. The two master faults limiting the gulf, at km 22 and 135 along the profile, are seismically active. A series of active faults observed along the profile correlate with the geologically mapped faults onshore western Peloponnese (see also Mariolakos *et al.*, 1985; IGME, 1989; Papanikolaou *et al.*, 2007; Papoulia and Makris, 2010). The previously described deep seismic activity is also presented at this profile between km 60 and 80.

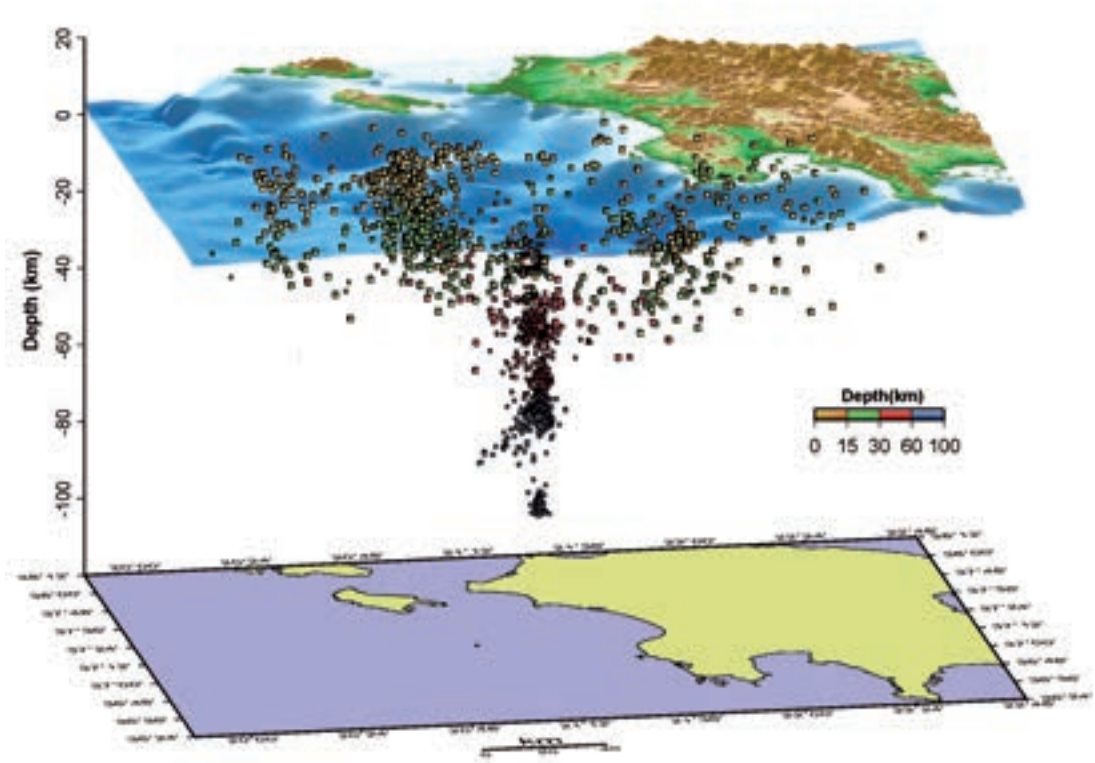

Fig. 16 - Depth distribution of located seismic events by the SEAHELLARC "amphibious" array and 3D velocity model defined from active seismic observations and 3D gravity modelling. The significant spatially confined seismicity extending to 90 km depth is associated with fracturing of the oceanic Ionian lithosphere during subduction. Further reading in the text.

6. Discussion

By deploying an "amphibious" network of 34 seismic stations with 3 or 4 channel each, we recorded the local seismic activity of the Kyparissiakos Gulf and south-western Peloponnese. In two months more than 3500 events were located. The seismicity defines major tectonic elements delineating thrust belts, normal and strike-slip faults. For the first time we could map in a fore-arc position subcrustal events extending to nearly 90 km depth close to the collision front of the continental backstop. This accentuates the fact that the subducted slab of the Ionian oceanic lithosphere below the crust of western Peloponnese is laterally affected and fractures by the laterally variable thickness of the continental crust. Due to the high accuracy in locating the micro earthquake events active deformation of the crust and lithosphere is clearly delineated, permitting a better understanding of the tectonic processes.

The Kyparissiakos basin is strongly affected by the dextral strike slip fault of Andravida. The western Hellenides, between the Cephalonia and Andravida dextral wrench faults, are extruded westwards sliding over Triassic evaporites and the deformation affects the sediments and the crust at its entire thickness (see also Makris and Papoulia, 2011). This causes significant thrusting and crustal shortening, generating transtensional basins along the wrench faults, like the rhombic pull apart basin NE of the Island of Strofades (Camera *et al.*, 2014), and transpressional uplifts, like that of the Strofades Island (see also Stiros, 2005).

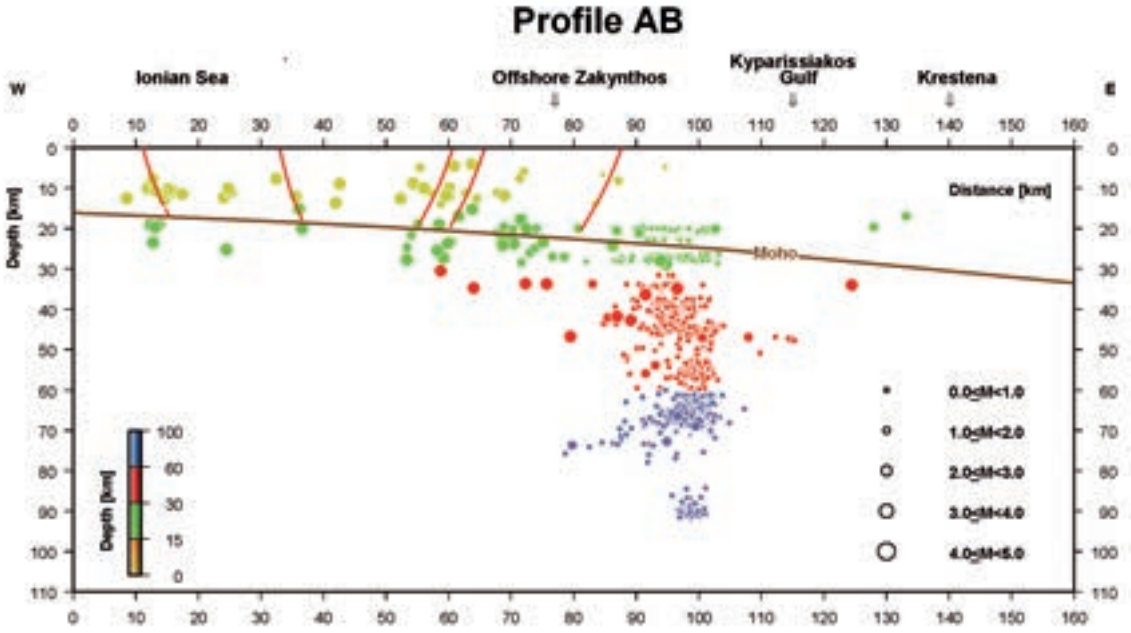

Fig. 17 - Depth distribution of recorded seismicity along profile AB. Moho depth is constrained by active seismic observations. Potential active faults from various sources (Mariolakos *et al.*, 1985; IGME, 1989; Papanikolaou *et al.*, 2007) are drawn along the profile.

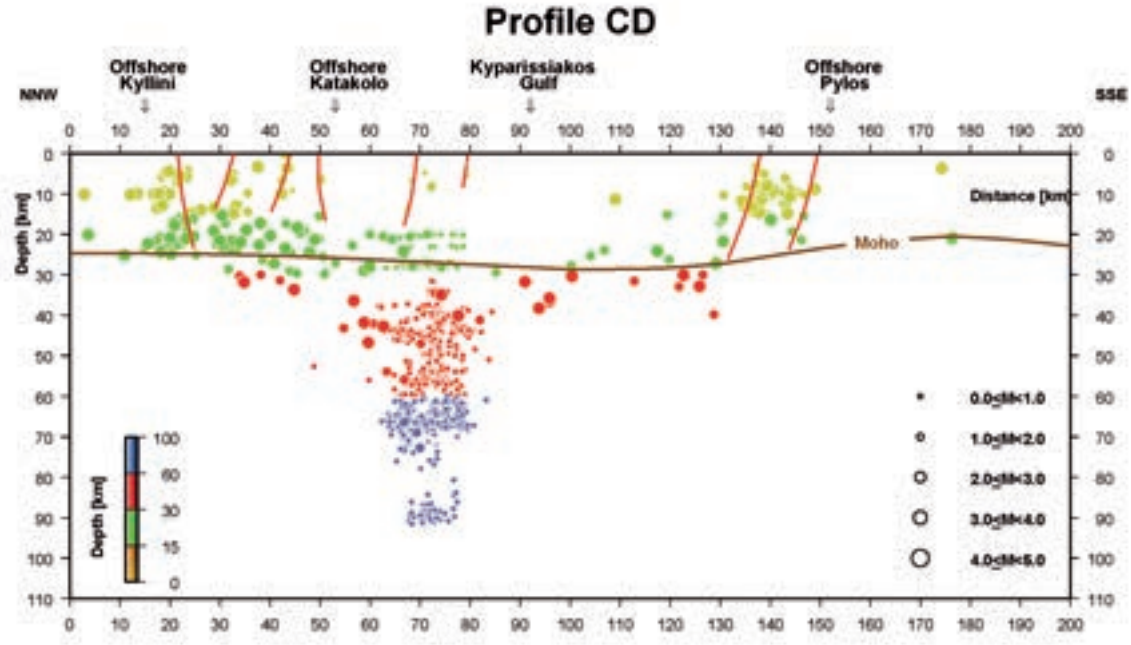

Fig. 18 - Depth distribution of recorded seismicity along profile CD. Moho depth is constrained by active seismic observations (Papoulia and Makris, 2010). Potential active faults from various sources (Mariolakos *et al.*, 1985; IGME, 1989; Papanikolaou *et al.*, 2007) are drawn along the profile.

The results of the present experiment contributed to the definition of a new seismogenic source model for the area of south-western Hellenic arc. It is now possible to define the seismic hazard accurately, providing objective constrains to engineering applications (see Slejko *et al*., 2014).

Acknowledgements. This paper is a contribution to the EC FP6 Project SEAHELLARC, contr. No. 37004. Data processing was performed by Ch. Fasulaka (GeoPro GmbH) and N. Levi (HCMR). Plots in GIS were prepared by V. Drakopoulou and Ch. Kiriakidou (HCMR). D. Ilinski, A. Martinenko, C. Soledade (GeoPro GmbH), P. Pagonis, G. Pappas, P. Kouraklis (HCMR) and G. Michaletos (NOA) participated in the field operations and data acquisition. The captain and crew of the R/V AEGAEO HCMR are acknowledged for their valuable help in OBS operations. Pier Luigi Bragato and Dario Slejko are acknowledged for their constructive review and useful comments that improved this paper.

REFERENCES

Birch F.; 1960: *The velocity of compressional waves in rocks to 10 kilobars. Pt. 1*. J. Geophys. Res., **65**, 1083-1102.

Birch F.; 1961: *The velocity of compressional waves in rocks to 10 kilobars. Pt. 2*. J. Geophys. Res., **66**, 2199-2224.

Camera L., Mascle J., Wardell N., Accettella D. and the SEAHELLARC team; 2014: *The Peloponnese continental margin from Zakynthos Island to Pylos: morphology and recent sedimentary processes*. Boll. Geof. Teor. Appl., **55**, 325-342, doi: 10.4430/bgta 0092.

Crosson R.S.; 1972: *Small earthquakes, structure and tectonics of the Puget Sound region*. Bull. Seismol. Soc. Am., **62**, 1133-1171.

Eberhart-Phillips D.; 1986: *Three-dimensional velocity structure in northern California Coast Range from inversion of local earthquake arrival times*. Bull. Seismol. Soc. Am., **76**, 1025-1052.

Eberhart-Phillips D.; 1990: *Three-dimensional P and S velocity structure in the Coalinga Region, California*. J. Geophys. Res., **95**, 15343-15363.

Geiger L.; 1912: *Probability method for the determination of earthquake epicentres from the arrival time only*. Bull. St. Louis Univ., **8**, 60-71.

IGME (Institute of Geology and Mineral Exploration); 1989: *Seismotectonic map of Greece, scale 1:500,000*. IGME, Athens, Greece.

Jackson J. and McKenzie D.; 1988: *Rates of active deformation in Aegean Sea and surrounding regions*. Basin Res., **1**, 121-128.

Kissling E., Ellsworth W.L., Eberhart-Phillips D. and Kradolfer U.; 1994: *Initial reference models in local earthquake tomography*. J. Geophys. Res., **99**, 19635-19646.

Klein F.; 1989: *User's Guide to HYPOINVERSE - 2000, a Fortran Program to solve for earthquake locations and magnitudes*. Open File Rep. 89-314, U.S.G.S., 123 pp.

Makris J.; 1977: *Geophysical investigations of the Hellenides*. Hamburg Geophys. Monogr., Univ. of Hamburg, Germany, Vol. 34, 98 pp.

Makris J. and Moeller L.; 1990: *An ocean bottom seismograph for general use. Technical requirements and applications*. In: Hoefeld J., Mitzlaff A. Polomsky S. (eds), Proc. Symp. Europe and the Sea, Hamburg, Germany, pp. 196-211.

Makris J. and Morelli C.; 1994: *The Bouguer gravity map of the Mediterranean Sea (IBCM-G)*. In: Hall J.K. (ed), IBMCM-supporting volume, 8th edn., Chapter 2, Jerusalem, Israel.

Makris J. and Papoulia J.; 2009: *Tectonic evolution of Zakynthos Island from deep seismic soundings: thrusting and its association with the Triassic evaporates,* In: Proc. Int. Symp. Evaporites, Zakynthos, Greece, pp. 47-54.

Makris J. and Papoulia J.; 2011: *Velocity modeling and mapping of sub-salt structures in sedimentary basins of western Greece using node technology.* In: Proc. 73rd EAGE Conf., Vienna, Austria, Extended abstract, pp. 75-79.

Makris J. and Papoulia J.; 2014: *The backstop between the Mediterranean Ridge and western Peloponnese, Greece: its crust and tectonization. An active seismic experiment with ocean bottom seismographs*. Boll. Geof. Teor. Appl., **55**, 249-279, doi: 10.4430/bgta0125.

Makris J. and Yegorova T.; 2006: *A 3-D density-velocity model between the Cretan Sea and Libya*. Tectonophys., **417**, 201-220.

Makris J., Morelli C. and Zanolla C.; 1998: *The Bouguer gravity map of the Mediterranean Sea (IBCM-G)*. Boll. Geof. Teor. Appl., **39**, 79-98.

Makris J., Papoulia J. and Yegorova T.; 2013: *A 3D density model of Greece constrained by seismic and gravity data*. Geophys. J. Int., **194**, 1-17.

Makropoulos C.; 1978: *The statistics of large earthquake magnitude and an evaluation of Greek seismicity*. PhD thesis, Edinburg Univ., Scotland, 193 pp.

Makropoulos C. and Burton P.W.; 1981: *A catalogue of the seismmicity in Greece and adjacent areas*. Geophys. J. R. Astron. Soc., **65**, 741-762.

Mariolakos I., Papanikolaou D. and Lagios E.; 1985: *A neotectonic geodynamic model of Peloponnesus based on: morphotectonics, repeated gravity measurements and seismicity.* Geol. Jahrb., **B50,** 3-17.

McKenzie D.; 1972: *Active tectonics in the Mediterranean region*. Geophys. J. R. Astron. Soc., **30**, 109-185.

Nafe J.E. and Drake Ch.L.; 1963: *Physical properties of marine sediments*. In: Hill M.N. (ed), The Sea, vol. 3, pp. 794-813.

Okal E.; 2008: *The generation of T waves by earthquakes*. Adv. Geophys., **49**, 1-65.

Papanikolaou D., Fountoulis J. and Metaxas Ch.; 2007: *Active faults, deformation rates and Quaternary paleogeography at Kyparissiakos Gulf (SW Greece) deduced from onshore and offshore data*. Quat. Int., **171-172**, 14-30.

Papazachos B.C. and Dimitriu P.P.; 1991: *Tsunamis in and near Greece and their relation to the earthquake focal mechanisms*. Nat. Hazards, **4**, 161-170.

Papazachos B. and Papazachou C.; 1997: *Earthquakes in Greece*. Editions Ziti, Thessaloniki, Greece, 304 pp.

Papoulia J. and Makris J.; 2004: *Microseismicity and active deformation of Messinia, SW Greece*. J. Seismol., **8**, 439-451.

Papoulia J. and Makris J.; 2010: *Tectonic processes and crustal evolution on/offshore western Peloponnese derived from active and passive seismics*. Bull. Geol. Soc. Greece, **43**, 357-367.

Papoulia J., Makris J., Mascle J., Slejko D. and Yalçiner A.; 2014: *The EU SEAHELLARC project: aims and main results*. Boll. Geof. Teor. Appl., **55**, 241-248, doi: 10.4430/bgta 0100.

Reasenberg P. and Oppenheimer D.; 1985: *FPFIT, FPPLOT and FPPAGE: FORTRAN computer programs for calculating and displaying earthquake fault-plane solutions*. Open File Rep. 85-739, U.S.G.S., Menlo Park, California, USA, 109 pp.

Slejko D., Santulin M. and Garcia J.; 2014: *Seismic hazard estimates for the area of Pylos and surrounding region (SW Peloponnese) for seismic and tsunami risk assessment*. Boll. Geof. Teor. Appl., **55**, 433-468, doi: 10.4430/bgta 0090.

Soloviev S.L.; 1990: *Tsunamigenic zones in the Mediterranean Sea*. Nat. Hazards, **3**, 183-202.

Stiros S.; 2005: *Geodetic evidence for mobilization of evaporates during the 1997 Strofades (W Hellenic Arc) 6.5 M_w earthquake*. J. Geophys. Eng., **2**, 111-117.

Thurber C.H.; 1983: *Earthquake location and 3D crustal structure in the Coyote Lake area, central California*. J. Geophys. Res., **88**, 8226-8236.

Urabe T. and Hirata N.; 1984: *A playback system for long-term analog tape recordings of ocean-bottom-seismographs*. J. Seismol. Soc. Jpn., **37**, 633-645.

Corresponding author: Joanna Papoulia
Institute of Oceanography, Hellenic Centre for Marine Research
46.7 km Athinon Souniou, 19013 Anavissos, Attiki, Greece
Phone: +30 2291 076370; fax: +30 2291 076323; e-mail: nana@ath.hcmr.gr.